*Electronic Supplementary Information (ESI) for*

# Origins of boron catalysis in peroxymonosulfate activation and advanced oxidation

Xiaoguang Duan[a,*], Wenlang, Li[b], Jian Kang[c], Wenjie Tian[a], Huayang Zhang[a], Shih-Hsin Ho[d], Zhimin Ao[b], Hongqi Sun[e], Shaobin Wang[a,c*]

[a] School of Chemical Engineering and Advanced Materials, The University of Adelaide, Adelaide, SA 5005, Australia

[b] School of Environmental Science and Engineering, Institute of Environmental Health and Pollution Control, Guangdong University of Technology, Guangzhou 510006, China

[c] Department of Chemical Engineering, Curtin University, Perth, WA 6845, Australia

[d] State Key Laboratory of Urban Water Resource and Environment, School of Environment, Harbin Institute of Technology, Harbin, China

[e] School of Engineering, Edith Cowan University, Joondalup, WA 6027, Australia

*Corresponding Authors:

xiaoguang.duan@adelaide.edu.au (X.D.)

shaobin.wang@adelaide.edu.au (S.W.)

**Text S1 Detailed synthesis procedure of the transition metal oxides.**

**Manganese dioxide ($MnO_2$)** was prepared by a hydrothermal method.[1] Manganese sulfate monohydrate (0.008 mol $MnSO_4 \bullet H_2O$) and an equal mole of ammonium persulfate ($(NH_4)_2S_2O_8$) were dissolved in ultrapure distilled water and stirred to form a homogeneous solution. Then the mixture was transferred into an 80 mL Teflon-lined stainless-steel autoclave and treated at 140 $^oC$ for 12 h. The product was filtered, washed with distilled water and finally dried in an oven at 60 $^oC$ overnight.

**Manganese(II, III) oxide ($Mn_3O_4$)** was synthesized by calcination of the obtained $MnO_2$ at 950 °C in air for 2 h to get $Mn_3O_4$.[2]

**Cobalt oxide ($Co_3O_4$)** was synthesized by a hydrothermal method.[3] Specifically, cobalt acetate tetrahydrate $Co(C_2H_3O_2)_2 \cdot 4H_2O$, 0.93 g) was dissolved in 70 mL $H_2O$, and then 10 mL of ammonium solution ($NH_3 \cdot H_2O$, 28%) was dropwise introduced into the solution. The mixture was transferred to a 120 mL Teflon-lined stainless-steel autoclave and treated at 180 $^oC$ for 12 h. The product was filtered, washed with distilled water and finally dried in an oven at 60 $^oC$ overnight.

**Synthesis of $Fe_3O_4$** was synthesised by a hydrothermal method.[4] $FeCl_3 \cdot 6H_2O$ (0.02 mol) and $FeCl_2 \cdot 4H_2O$ (0.01 mol) were dissolved in 80 mL of ultrapure water, followed by 1 h stirring. With stirring, 28% ammonia solution was added dropwisely at a rate of 0.5 mL/min with nitrogen bubbling (40 mL/min) to keep solution at pH = 10. The mixed solution was then transferred into a Teflon-lined autoclave (120 mL) and treated at 180 °C in an oven for 18 h. The product was filtered, washed with distilled water and finally dried in an oven at 60 $^oC$ overnight.

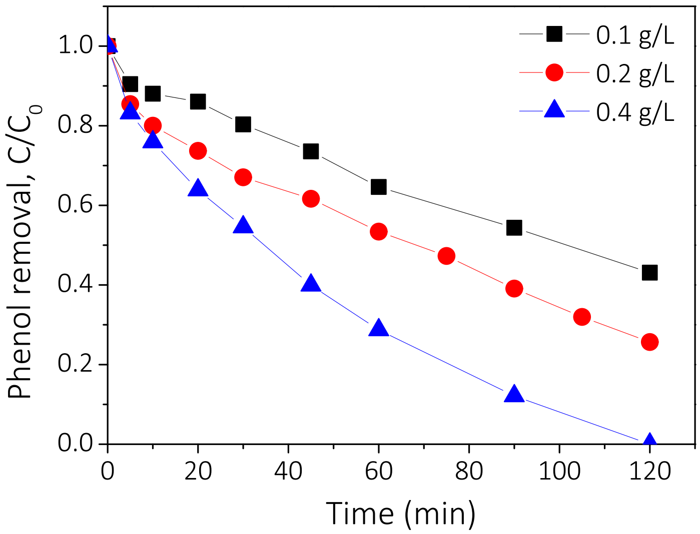

**Figure S1.** The effect of catalyst loading on catalytic phenol oxidation. (Experimental conditions: phenol = 0.1 mM, PMS = 3.3 mM, temperature = 25 °C.)

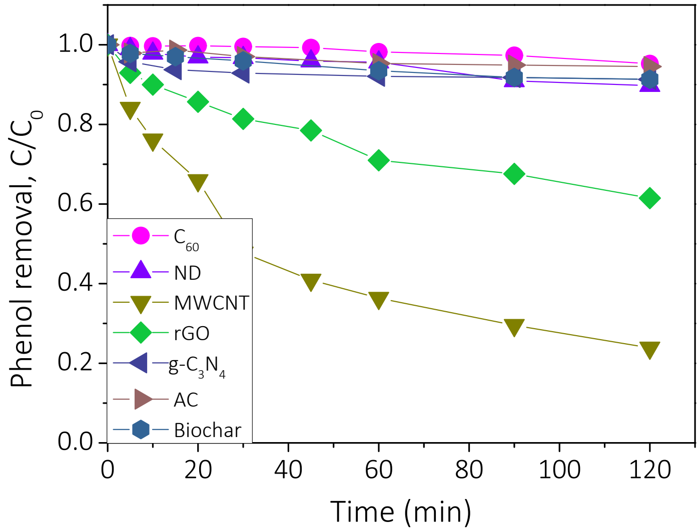

**Figure S2.** Catalytic performance of different carbocatalysts for PMS activation and phenol oxidation. (Experimental conditions: phenol = 0.1 mM, catalyst= 0.2 g/L, PMS = 3.3 mM, temperature = 25 °C.)

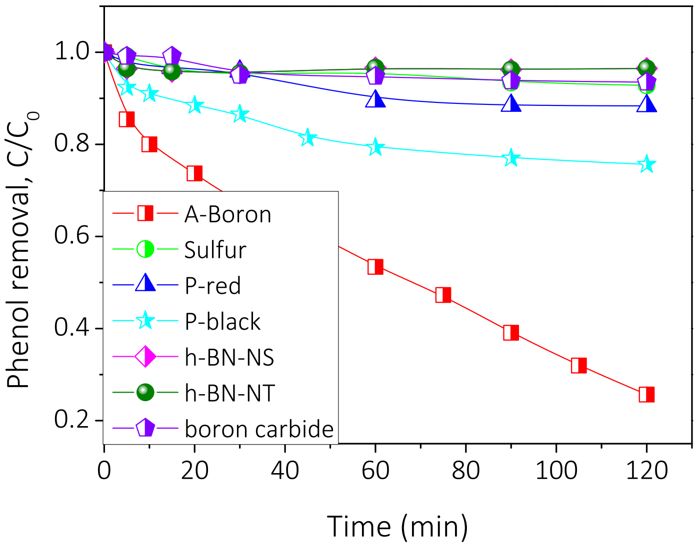

**Figure S3.** Catalytic performances of different metal-free non-carbon materials for PMS activation and phenol oxidation. (Experimental conditions: phenol = 0.1 mM, catalyst= 0.2 g/L, PMS = 3.3 mM, temperature = 25 °C.)

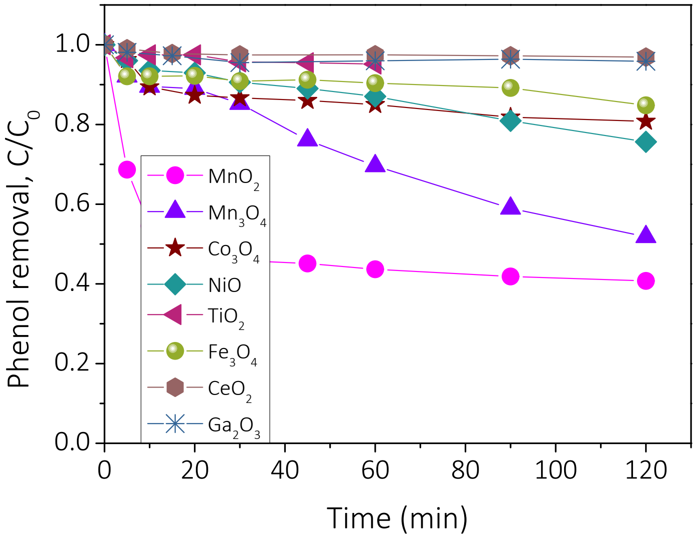

**Figure S4.** Catalytic performances of different transition metal oxides for PMS activation and phenol oxidation. (Experimental conditions: phenol = 0.1 mM, catalyst= 0.2 g/L, PMS = 3.3 mM, temperature = 25 °C.)

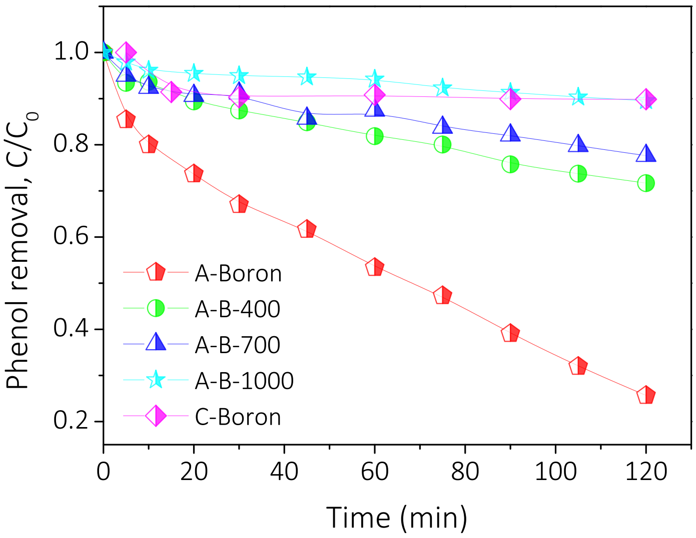

**Figure S5.** Catalytic performances of different boron materials for PMS activation and phenol oxidation. (Experimental conditions: phenol = 0.1 mM, catalyst= 0.2 g/L, PMS = 3.3 mM, temperature = 25 °C.)

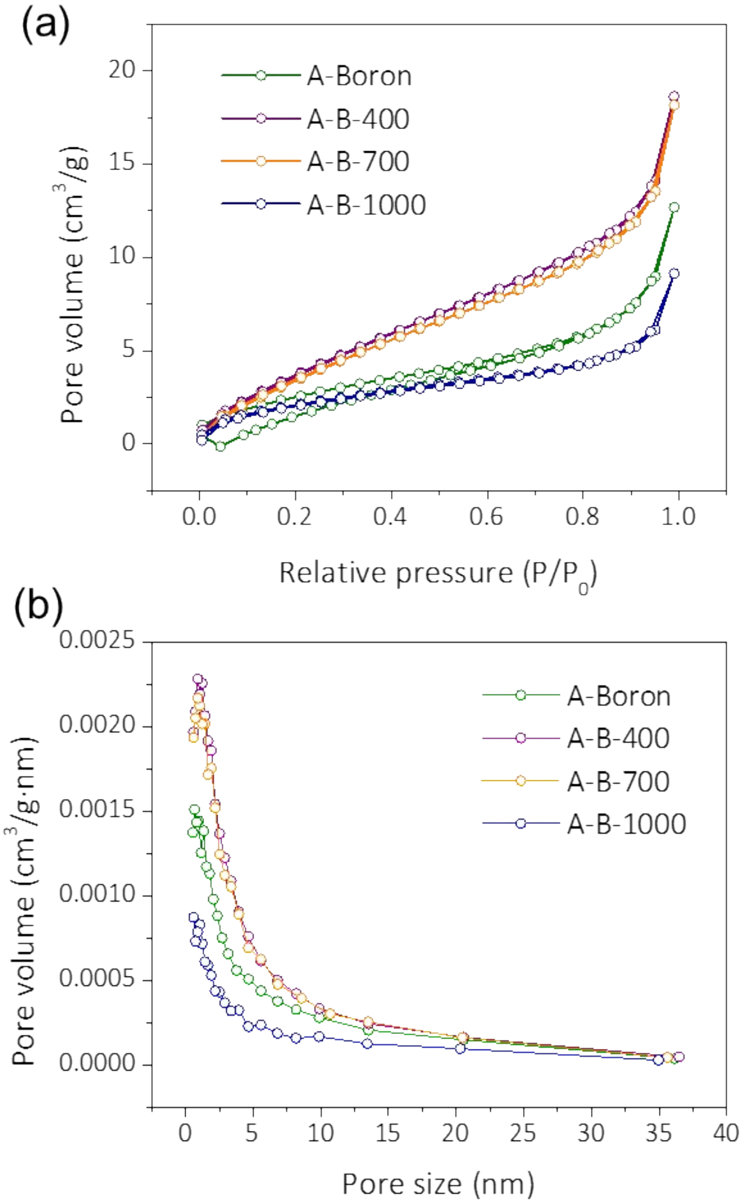

**Figure S6.** (a) Nitrogen adsorption isotherms and (b) pore size distribution of the boron samples.

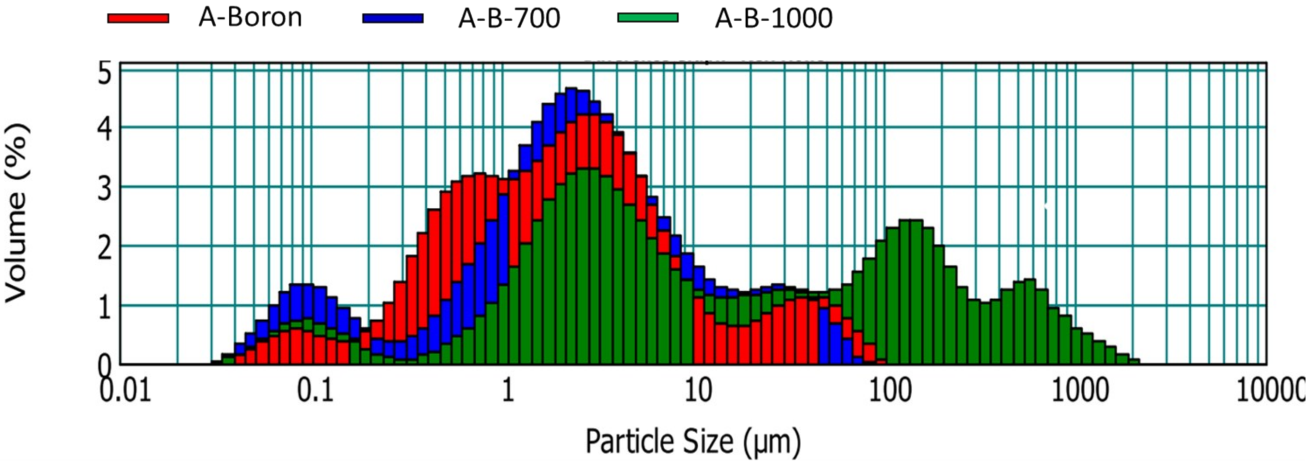

**Figure S7.** Particle size distribution analysis of different boron samples.

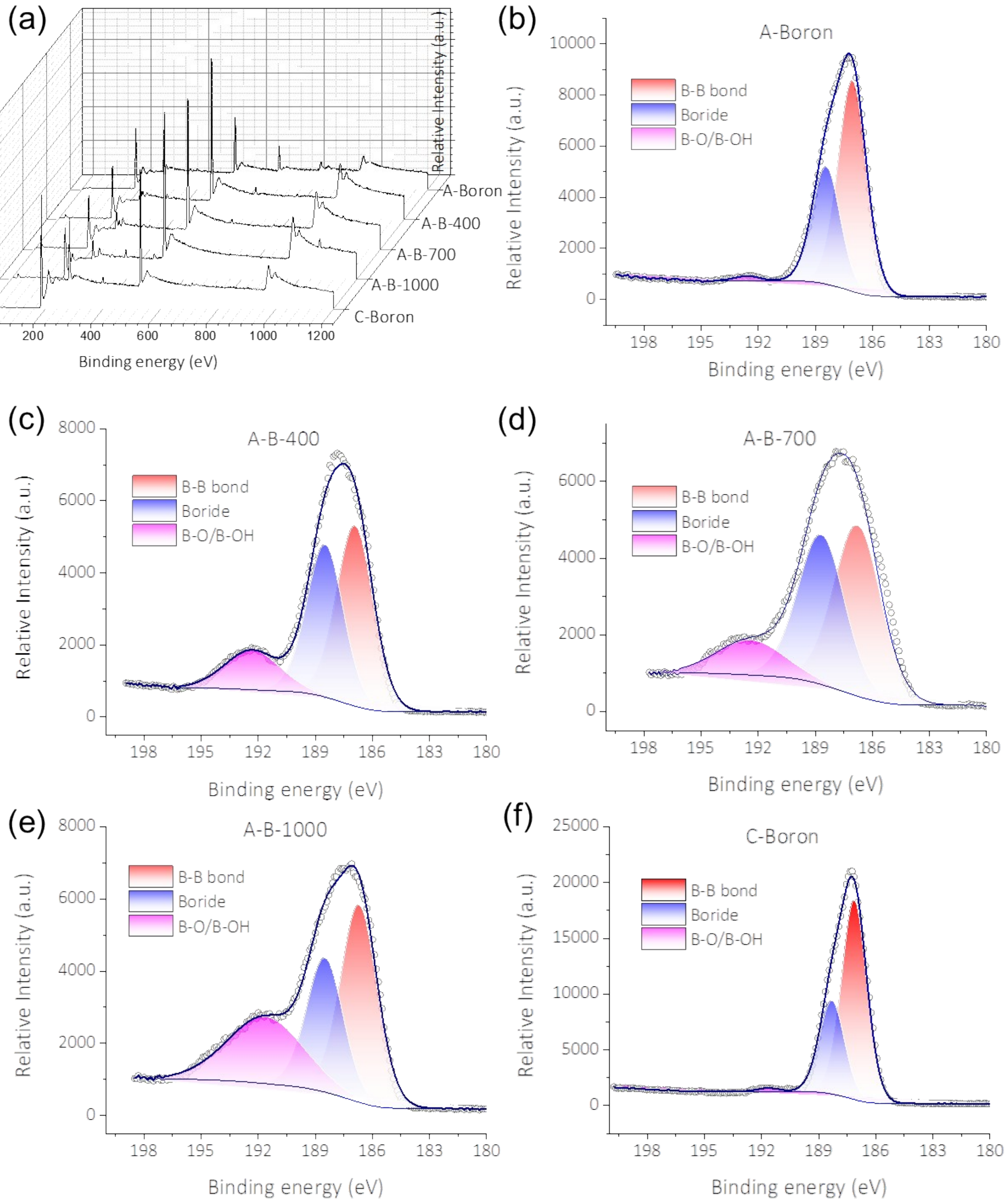

**Figure S8.** (a) XPS surveys of the boron samples. High-resolution XPS spectra of B 1s peak and fitting compounds of (b) A-Boron, (c) A-B-400, (d) A-B-700, (e) A-B-1000, and (f) C-Boron.

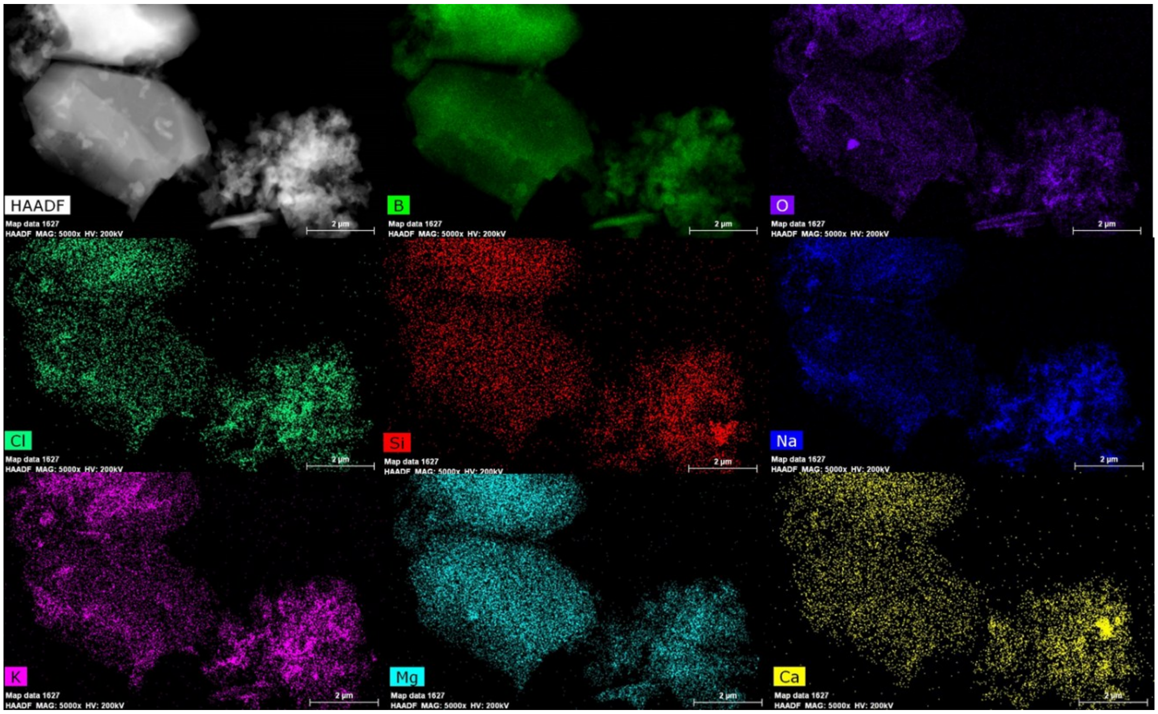

**Figure S9.** High-angle annular dark-field (HAADF) and EDX elemental mapping of A-Boron.

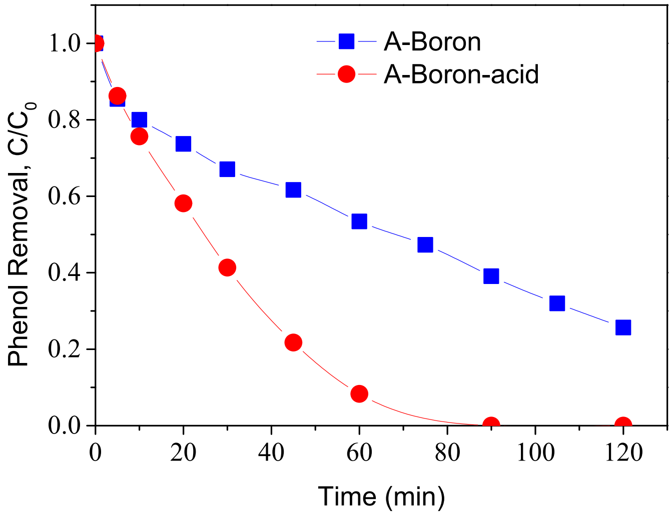

**Figure S10.** Comparison of the reactivities before (A-Boron) and after acid washing (A-Boron-acid, 1 wt.% HCl washing for 6 h). (Experimental conditions: phenol = 0.1 mM, catalyst= 0.2 g/L, PMS = 3.3 mM, temperature = 25 °C)

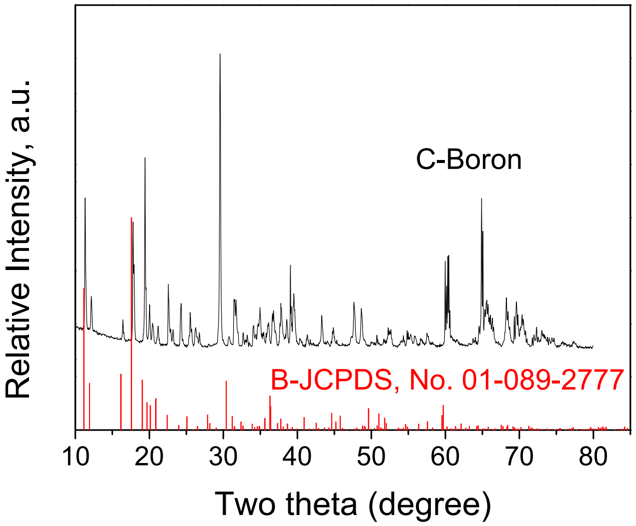

**Figure S11.** Comparison of XRD spectrum of C-Boron with Boron JCPDS card.

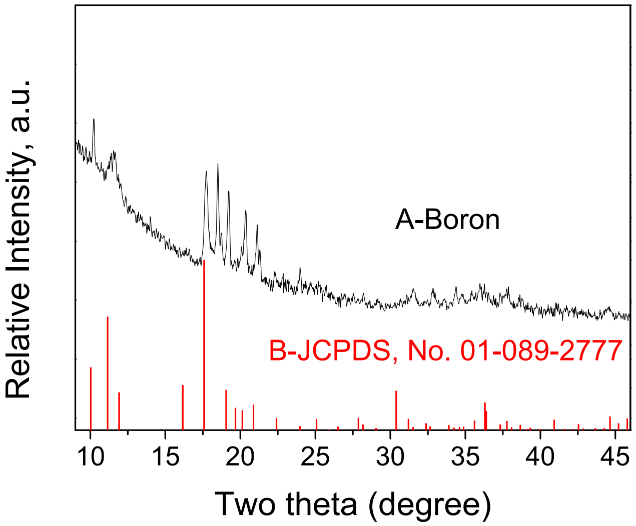

**Figure S12.** Comparison of XRD spectrum of A-Boron with Boron JCPDS card.

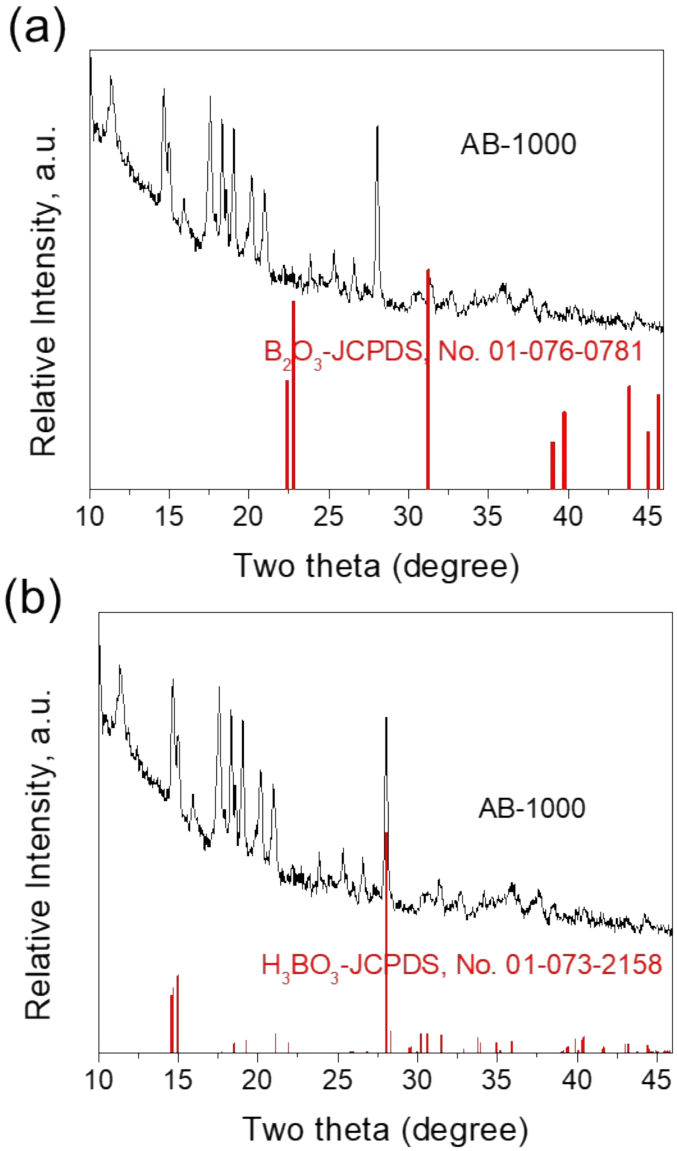

**Figure S13.** Comparison of XRD spectrum of A-B-1000 with JCPDS cards of (a) $B_2O_3$ and (b) $H_3BO_3$.

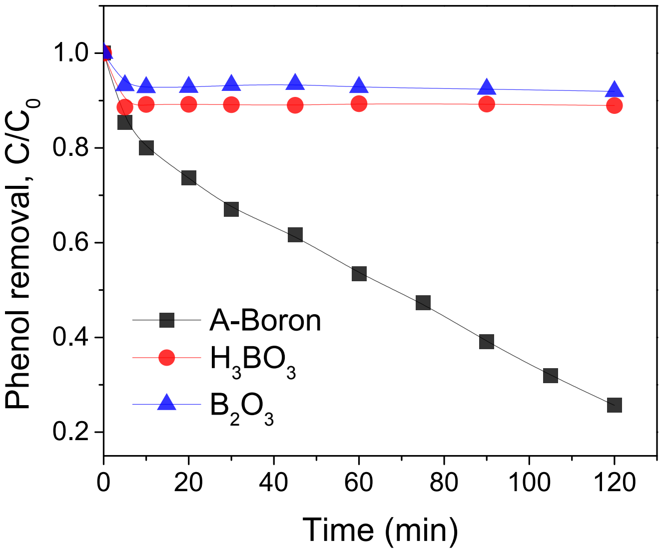

**Figure S14.** Reactivity comparison of A-Boron with $B_2O_3$ and $H_3BO_3$. (Experimental conditions: phenol = 0.1 mM, catalyst= 0.2 g/L, PMS = 3.3 mM, temperature = 25 °C)

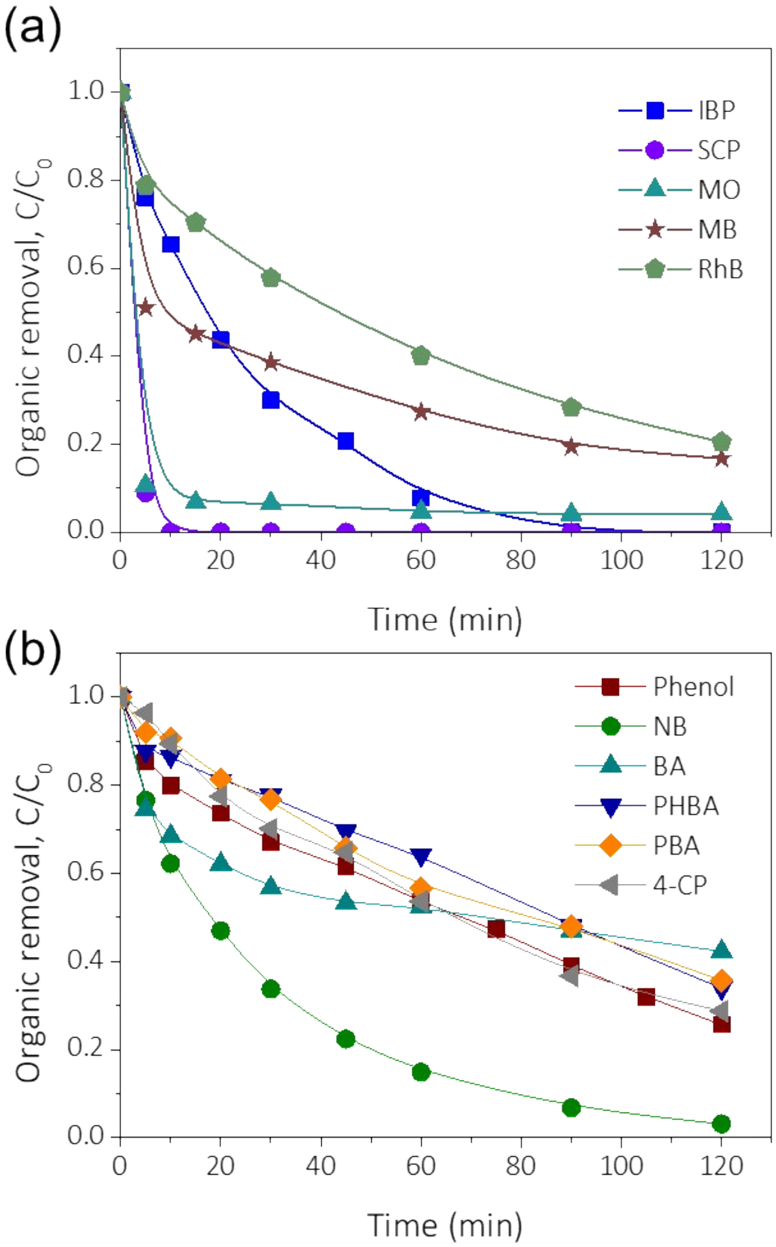

**Figure S15.** Catalytic degradation of various organic contaminants by A-Boron/PMS system. (Experimental conditions: organics = 0.1 mM, catalyst= 0.2 g/L, PMS = 3.3 mM, temperature = 25 °C)

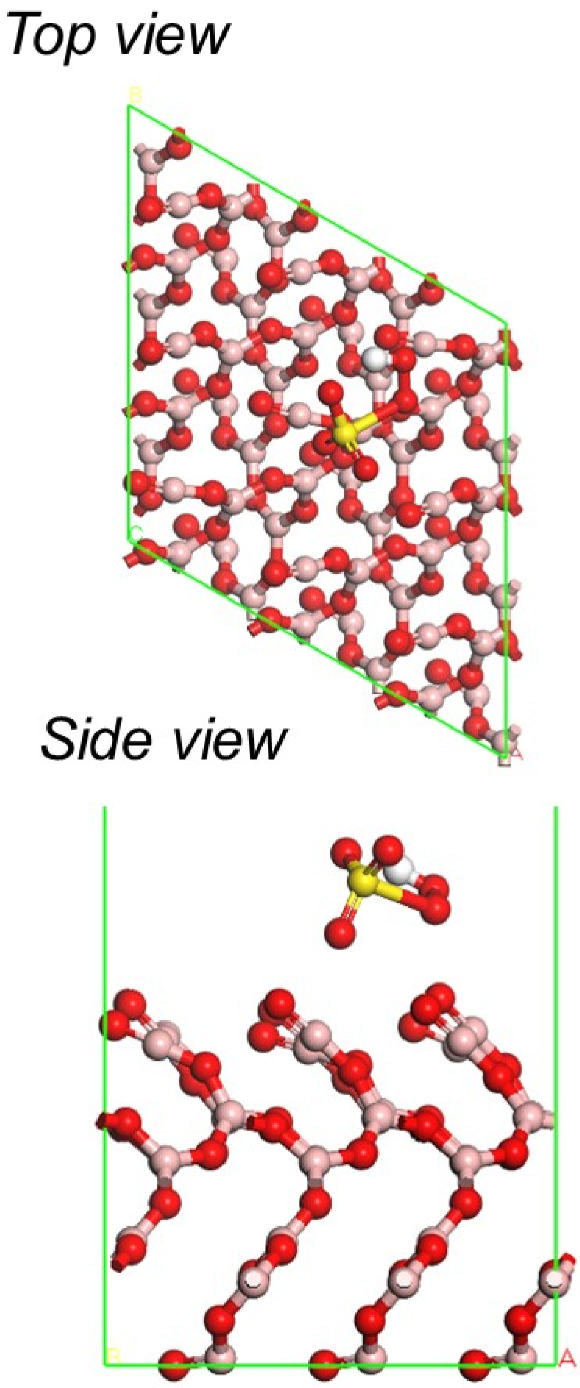

**Figure S16.** Illustration of PMS adsorption on the (0 0 1) termination of $B_2O_3$.

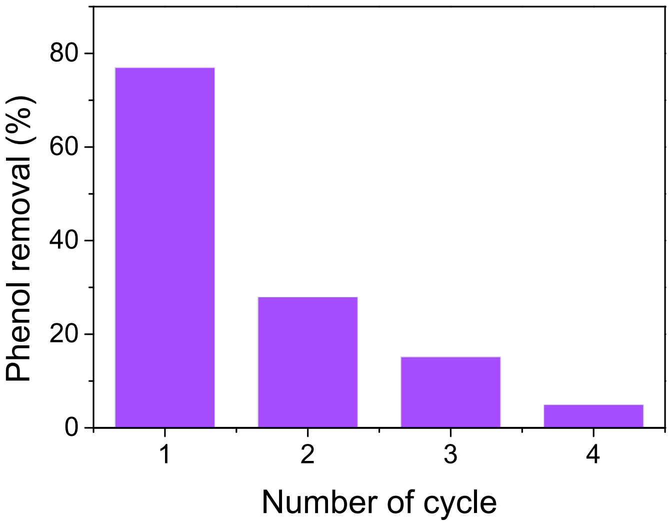

**Figure S17.** Stability of A-Boron for PMS activation and catalytic phenol oxidation for 180 min in multiple runs. (Experimental conditions: phenol = 0.2 mM, catalyst= 0.2 g/L, PMS = 3.3 mM, temperature = 25 °C)

Top view

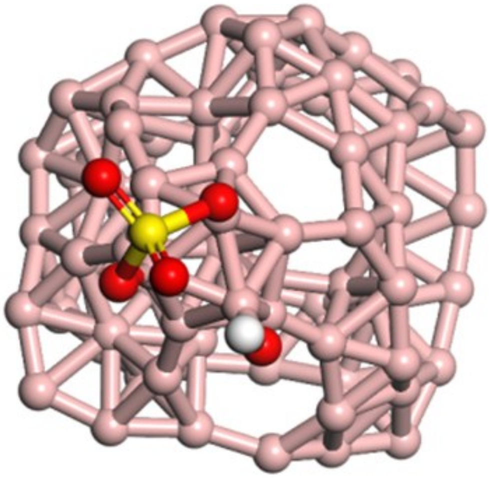

Side view

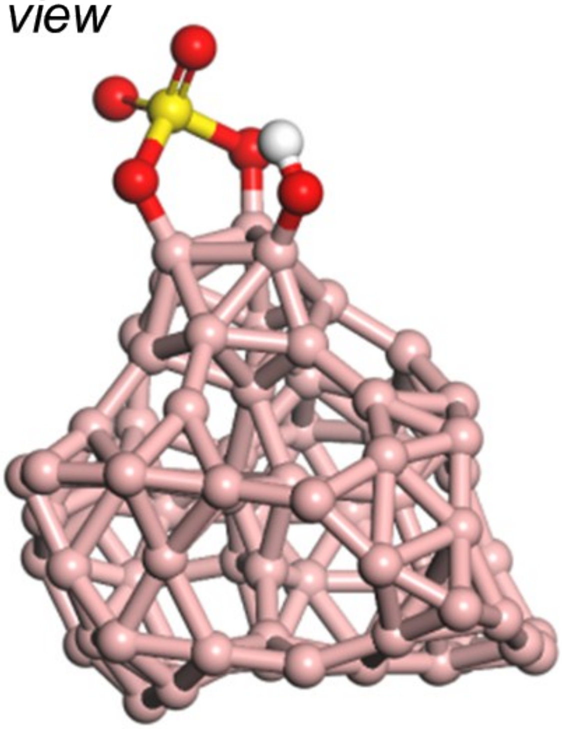

**Figure S18.** Illustration of PMS dissociate over a structurally relaxed B75 cluster.

**Table S1.** Summary of electron transfer from boron to activated PMS and the associated adsorption energies.

| Boron Terminations or Structure | Charge transfer to OH (e) | Charge transfer to $SO_4$ (e) | Total charge transfer (e) | Adsorption energy (eV) |
|---|---|---|---|---|
| (1 0 0) | 0.180 | 0.644 | 0.824 | -7.58 |
| (1 0 1) | 0.194 | 0.794 | 0.988 | -10.6 |
| (1 1 0) | 0.061 | 0.657 | 0.718 | -7.18 |
| B75 cluster | 0.163 | 0.716 | 0.879 | -9.58 |
|  | Charge transfer to O (e) | Charge transfer to $HSO_4$ (e) | Total charge transfer (e) |  |
| (0 0 1) | 0.506 | 0.282 | 0.788 | -7.91 |
| (1 1 1) | 0.371 | 0.295 | 0.666 | -7.34 |

## References

1. X. Wang and Y. D. Li, *Chem.-Eur. J.*, 2003, **9**, 300-306.
2. E. Saputra, S. Muhammad, H. Q. Sun, H. M. Ang, M. O. Tade and S. B. Wang, *Appl. Catal. B*, 2013, **142**, 729-735.
3. Y. J. Yao, Z. H. Yang, H. Q. Sun and S. B. Wang, *Ind. Eng. Chem. Res.*, 2012, **51**, 14958-14965.
3. Y. X. Wang, H. Q. Sun, H. M. Ang, M. O. Tade and S. B. Wang, *Chem. Eng. J.*, 2014, **245**, 1-9.